

Highly Accurate Robot Calibration Using Adaptive and Momental Bound with Decoupled Weight Decay

Tinghui Chen Student Member, *IEEE* and Shuai Li, *Senior Member, IEEE*

Abstract—Within the context of intelligent manufacturing, industrial robots have a pivotal function. Nonetheless, extended operational periods cause a decline in their absolute positioning accuracy, preventing them from meeting high precision. To address this issue, this paper presents a novel robot algorithm that combines an adaptive and momental bound algorithm with decoupled weight decay (AdaModW), which has three-fold ideas: a) adopting an adaptive moment estimation (Adam) algorithm to achieve a high convergence rate, b) introducing a hyperparameter into the Adam algorithm to define the length of memory, effectively addressing the issue of the abnormal learning rate, and c) interpolating a weight decay coefficient to improve its generalization. Numerous experiments on an HRS-JR680 industrial robot show that the presented algorithm significantly outperforms state-of-the-art algorithms in robot calibration performance. Thus, in light of its reliability, this algorithm provides an efficient way to address robot calibration concerns.

Index Terms—Industrial robot, Kinematic calibration, Adaptive moment estimation with decoupled weight decay algorithm, Positioning accuracy.

I. INTRODUCTION

Industrial robots have advantages like fast operation speed, high efficiency, and flexible control systems making them increasingly significant in intelligent manufacturing [1]-[16]. However, the demand for operational accuracy and work efficiency of robots is increasing as the applications of industrial robots continue to expand [19]-[38]. The robot positioning accuracy is affected by various factors, including the machining assembly, elastic or inelastic deformation, wear, collisions, etc. The total errors of a robot are composed of kinematic errors and dynamic errors, and the dynamic errors constitute less than 10% [39]-[51]. Thus, we concentrate on addressing the kinematic errors through kinematic calibration.

Aiming to achieve high-efficiency kinematic error calibration for robots, pioneering scholars have conducted numerous in-depth research [52]-[63]. For instance, Kwon et al. [64] identify the robotic kinematic parameters with the least square (LS) algorithm, which achieves a significant reduction in model bias. Fin *et al.* [65] build a robot kinematic error model based on an extended Kalman filter (EKF) algorithm. Empirical studies implemented on a novel 5-DOF hybrid robot demonstrate that the EKF algorithm evidently outperforms the least square algorithm in calibration accuracy and robustness. Lou *et al.* [66] propose a hybrid calibrator by incorporating a differential evolution (DE) algorithm into a Levenberg-Marquardt (LM) for a FANUC M710ic/50 industrial robot calibration. Experimental results show that the proposed calibrator can reduce the positioning error of the robot from 0.994mm to 0.262mm. Chen *et al.* [67] present an improved beetle swarm optimization (BSO) algorithm to identify an industrial robot's kinematic parameters, achieving a huge reduction of positioning error from 2.95mm to 0.2mm. Mao *et al.* [68] approximate the minimax issue of the robot calibration as a sequential quadratic programming (SQP) issue. Then, the SQP issue is addressed with a primal-dual sub-gradient algorithm to achieve a fast convergence rate. Numerous experimental studies conducted on an ABB IRB 14000 robot demonstrate the proposed method can successfully enhance its calibration accuracy.

In general, the above-mentioned algorithms enable the enhancement of the robot positioning accuracy to a large extent. However, they frequently encounter issues like local optimum, poor stability, slow convergence rate, etc., which damage the calibration performance of the robots. Hence, this paper presents a novel algorithm that combines an adaptive and momental bound algorithm with decoupled weight decay (AdaModW). It contains the following ideas:

- a) Adopting an adaptive moment estimation (Adam) algorithm to achieve a high convergence rate.
- b) Introducing a hyperparameter into the Adam algorithm to define the length of memory, effectively addressing the issue of the abnormal learning rate.
- c) Interpolating a weight decay coefficient to address the inadequacy of weight decay and improve its generalization.

Key contributions of this paper are below:

- a) An efficient AdaModW algorithm. It interpolates a learning rate control hyperparameter and a weight decay coefficient into an Adam algorithm, achieving a high convergence rate and calibration accuracy.
- b) Empirical studies conducted on an HRS-JR680 industrial robot demonstrate the superiority of the AdaModW algorithm in calibration accuracy compared with state-of-the-art algorithms.

Section II briefly describes the preliminaries. The proposed methodology is detailed in Section III. Section IV discusses the experimental results. Section V concludes the paper and gives several future works.

II. PRELIMINARIES

The most classical kinematics model, i.e., the D-H model, consists of four parameters, i.e., link twist angle (α_i), joint angle (θ_i), link length (a_i), and d_i (link offset) [1]. Table I lists the nominal D-H parameters of the adopted robot. The transformation matrix of the D-H model is given as:

$$\Gamma_i = \begin{bmatrix} \cos \theta_i & -\sin \theta_i \cos \alpha_i & \sin \theta_i \sin \alpha_i & a_i \cos \theta_i \\ \sin \theta_i & \cos \theta_i \cos \alpha_i & -\cos \theta_i \sin \alpha_i & a_i \sin \theta_i \\ 0 & \sin \alpha_i & \cos \alpha_i & d_i \\ 0 & 0 & 0 & 1 \end{bmatrix}, \quad (1)$$

Then, the end-effector of the robot is described as:

$$\Gamma = \Gamma_1 \Gamma_2 \Gamma_3 \cdots \Gamma_6. \quad (2)$$

The kinematic model deviation can be represented as:

$$d\Gamma = \begin{bmatrix} \Delta H & \Delta O \\ 0 & 1 \end{bmatrix}, \quad (3)$$

where ΔH is the rotation matrix error of the robot, and ΔO is the position error of the robot. Note that the holomorphic differential of Γ_i can be described as:

$$d\Gamma_i = \frac{\partial \Gamma_i}{\partial \alpha_i} \Delta \alpha_i + \frac{\partial \Gamma_i}{\partial \theta_i} \Delta \theta_i + \frac{\partial \Gamma_i}{\partial a_i} \Delta a_i + \frac{\partial \Gamma_i}{\partial d_i} \Delta d_i. \quad (4)$$

According to (2), (3) and (4), the pose error model is given as:

$$Error = \begin{bmatrix} U_1 & U_2 & U_3 & U_4 \end{bmatrix} \begin{bmatrix} \Delta \alpha \\ \Delta a \\ \Delta d \\ \Delta \theta \end{bmatrix} = U \Delta g, \quad (5)$$

where U refers to the Jacobian matrix, and Δg is the D-H parameter deviations vector. Note that the dimension of the D-H parameter vector is set as 24, i.e., $o=24$.

III. KINEMATIC PARAMETERS IDENTIFICATION

A. AdaModW Algorithm

In this part, we introduce the AdaModW algorithm and its unique features. Initially, we set the dynamic upper bound to avoid the adaptive learning rate increasing too fast and surpassing the historically largest one [69]. This method significantly enhances the stability of the model and ensures equilibrium in the learning process. Moreover, this paper decreases model complexity and avoids overfitting by decoupling weight decay, thereby enhancing its generalizability [70]. In contrast to L_2 regularization, weight decay operates directly on the parameter updates, which penalizes large weights and maintains optimized performance. The specific details of the AdaModW algorithm are as follows:

a) First-order moment estimate. Calculate the exponential moving average of the gradient:

$$m_t = \beta_1 m_{t-1} + (1 - \beta_1) U_t, \quad (6)$$

where m_t represents the first-order moment estimate at the t -th iteration, U_t is the gradient matrix at the t -th iteration (the Jacobian matrix in this paper), and β_1 is the decay weight of the first-order moment estimate.

b) Second-order moment estimate. Calculate the exponential moving average of the squared gradient:

$$z_t = \beta_2 z_{t-1} + (1 - \beta_2) U_t^2, \quad (7)$$

where z_t denotes the second-order moment estimate at the t -th iteration, U_t^2 is the square of the gradient at the t -th iteration, β_2 is the decay weight of the second-order moment estimate.

c) Biases calibration. According to the literature [30], m and v are inclined to zero at the beginning of training, causing the distance estimate to be biased towards zero. Consequently, the corrections for the biases are required, which are formulated as:

$$\hat{m}_t = \frac{m_t}{1 - \beta_{1,t}}, \hat{z}_t = \frac{z_t}{1 - \beta_{2,t}}, \quad (8)$$

where \hat{m}_t and \hat{z}_t denote the corrected m_t and z_t , respectively.

d) Update rules. The D-H parameters are updated as:

$$g_t = g_{t-1} - \frac{\eta}{\sqrt{\hat{z}_t} + \sigma} \hat{m}_t, \quad (9)$$

where η is the learning rate, and σ is a tiny constant that prevents division by zero. Then, this work defines the adaptive learning rate as:

$$\kappa_t = \frac{\eta_t}{\sqrt{\hat{z}_t} + \sigma}, \quad (10)$$

e) Adjusting adaptive learning rate. Motivated by the exponential moving average, we update the adaptive learning rate by computing its average. Specifically, it consists of the following operations:

$$b_t = \beta_3 b_{t-1} + (1 - \beta_3) \kappa_t, \quad (11)$$

where b_t is the adjusted value at the t -th iteration, and β_3 denotes a discount factor for controlling b_t . Notably, the current b_t represents an interpolation between the current κ_t and the prior b_{t-1} . The data's mean range in the exponential moving average is $1/\beta_3$, as deduced from its expanded form. For instance, with β_3 set to 0.9, 0.99, and 0.999, the average range spans 10, 100, and 1000 periods, respectively. The other settings for β_3 follow the same logic.

Note that, (16) has another expression, which can describe b_t as an exponential weighted moving average. Thus, b_t can also be formulated as:

$$b_t = (1 - \beta_3) [b_{t-1} + \beta_3 b_{t-2} + \beta_3^2 b_{t-3} + \dots + \beta_3^{t-1} b_0]. \quad (12)$$

Based on (17), b_t retains a ‘long-term memory’ of the set $\{b_{t-1}, \dots, 0\}$. Notably, b_0 is set to 0 and is not subject to bias correction.

Then, to prevent excessively high learning rates, we update the adaptive learning rate through a bounding operation, i.e., by comparing it with the current adjusted value b_t . Hence, it can be reformulated as:

$$\hat{\kappa}_t = \min(\kappa_t, b_t), \quad (13)$$

where $\hat{\kappa}_t$ represents the ultimate learning rate calculated by bounding operation. Hence, the training process can effectively constrain the output by the adjusted value. Then, (14) can be rewritten as:

$$g_t = g_{t-1} - \hat{\kappa}_t \hat{m}_t, \quad (14)$$

e) Decoupled weight decay strategy. It is to implement weight decay directly on the parameter updates. Hence, (19) is updated as:

$$g_t = g_{t-1} - \hat{\kappa}_t (\hat{m}_t + \zeta g_{t-1}), \quad (15)$$

where ζ denotes the weight decay coefficient.

IV. EXPERIMENTS AND RESULTS

A. General Settings

Evaluation Metrics. To validate the experiments, three evaluation metrics, i.e., mean square error (RMSE), mean error (MEAN), and maximum error (MAX) are employed, which can be given as [1], [71]-[78]:

$$\begin{aligned} MAX &= \max(|C_i - \hat{C}_i(g)|), i = 1, 2, \dots, n, \\ MEAN &= \frac{1}{n} \sum_{i=1}^n |C_i - \hat{C}_i(g)|, \\ RMSE &= \sum_{i=1}^n \left(\sqrt{\frac{1}{n} (C_i - \hat{C}_i(g))^2} \right). \end{aligned}$$

where n refers to the sample count, C_i is the measured wire length, and $\hat{C}_i(h)$ represents the nominal wire length

Experimental Setup. It contains an HSR-JR680 industrial robot, a dedicated robot controller, a cable-extension transducer, a cable-extension indicator, and a computer.

Experimental Process. Firstly, 2000 sample points are selected in the robot’s workspace and measured with a cable-extension transducer. Note that the collected sample points are evenly distributed across the entire workspace of the robot. Afterwards, the proposed AdaModW algorithm is adopted to optimize the D-H parameter vector by training the selected samples, aiming to greatly decrease the robot positioning error.

B. Comparisons

Compared results. In this part, this paper conducts several experiments to verify the performance of the proposed algorithm. Table II details the compared algorithms. Table III illustrates the calibration accuracy before calibration and after calibration by M1-8. Table IV shows the iteration count and computational efficiency of M1-8. Fig. 2 depicts the experimental results in the calibration accuracy of M1-8. Fig. 3 shows the training processes and total time costs of M1-8. Fig. 4 illustrates the positioning accuracy of all algorithms. The deviations of the kinematic parameters are recorded in Table V. From the above results, we obtain the following findings:

- a) In the realm of calibration accuracy, AdaModW surpasses other algorithms.** As shown in Table III and Fig. 2, it is evidently seen that M8, i.e., the presented algorithm, significantly advances robot calibration accuracy, demonstrating a superior performance advantage over other cutting-edge algorithms. For instance, the RMSE achieved by M8 is 0.646mm, which is 23% less than M1’s 0.839mm, 53.36% less than M2’s 1.385mm, 21.79% less than M3’s 0.826mm, 5.28% less than M4’s 0.682mm, 1.07% less than M5’s 1.07mm, 4.86% less than M6’s 0.679mm, 14.55% less than M7’s 0.756mm. Considering MEAN, the outputs by M1-8 are 0.739mm, 1.288mm, 0.713mm, 0.59mm, 0.562mm, 0.588mm, 0.662mm, and 0.522mm, respectively. Hence, M1’s MEAN is also considerably lesser than that of its counterparts. Moreover, M8’s MAX is 1.011mm, which is 38.17%, 61.46%, 36.25%, 36.25%, 13.07%, 2.03%, 10.13%, and 24.33% than that of M1-7.
- b) AdaModW boasts a remarkably rapid convergence rate.** For instance, from Table IV and Fig. 3, M1-7 require 58, 13, 82, 60, 68, 22, and 15 iterations, respectively, to achieve convergence in RMSE. However, M8 converges to RMSE within only 10 iterations, far fewer than its peers. The high convergence rate may be attributed to the innovative learning scheme introduced in Section III.
- c) AdaModW’s computational efficiency is competitive.** For instance, From Table IV, M8 takes 10.3 seconds to converge in RMSE, which is 70.82%, 11.21%, 50.72%, 68.88%, 67.81%, 77.75%, and 36.02% lower than that of M1-9, respectively. Thus, M8 achieves a competitive level of computational efficiency.

TABLE I. HRS JR680 INDUSTRIAL ROBOT D-H PARAMETERS.

Joint i	1	2	3	4	5	6
$\alpha_i/^\circ$	-90	0	-90	90	-90	0
a_i/mm	250	900	-205	0	0	0
d_i/mm	653.5	0	0	1030.2	0	200.6
$\theta_i/^\circ$	0	-90	180	0	90	0

TABLE II. COMPARED ALGORITHMS.

No.	Description
M1	The Genetic Algorithm (GA) is introduced in [71].
M2	The EKF algorithm in [72].
M3	The BSO algorithm is introduced in [67].
M4	The LM algorithm [73] is frequently employed for robot calibration, which can effectively address the issue of over-fitting.
M5	The improved whale optimization algorithm (IWOA) [75] integrates deep search strategies with the whale optimization algorithm (WOA), enhancing its global search capabilities significantly.
M6	Radial basis function neural network (RBFNN) is introduced in [76].
M7	The Adam algorithm combines the concepts of momentum and adaptive learning rates, ensuring efficient computational performance [79].
M8	The proposed AadModW algorithm.

TABLE III. THE CALIBRATION ACCURACY BEFORE CALIBRATION AND AFTER CALIBRATION BY M1-8.

Models	RMSE/mm	MEAN/mm	MAX/mm
BC	4.56	4.45	5.81
M1	0.839±7.3E-3	0.739±8.1E-3	1.635±8.2E-2
M2	1.385±1.1E-2	1.288±1.2E-2	2.623±1.0E-2
M3	0.826±1.3E-2	0.713±2.2E-2	1.586±2.1E-2
M4	0.682±2.1E-2	0.590±2.1E-2	1.163±2.1E-2
M5	0.653±2.0E-2	0.562±1.8E-2	1.032±1.2E-2
M6	0.679±1.0E-2	0.588±1.2E-2	1.125±9.6E-3
M7	0.756±1.1E-2	0.662±8.2E-3	1.336±7.9E-3
M8	0.646±1.2E-2	0.552±1.1E-2	1.011±9.2E-3

TABLE IV. THE TIME COSTS AND ITERATION COUNTS OF M1-8.

Models	Iterations (RMSE)	Time/s (RMSE)
M1	58	35.3±2.11
M2	13	11.6±1.63
M3	82	20.9±2.76
M4	60	33.1±0.91
M5	68	32.0±1.07
M6	22	46.3±2.36
M7	15	16.1±1.74
M8	10	10.3±1.5

TABLE V. D-H PARAMETERS AFTER M9 CALIBRATION.

Joint i	$\alpha_i/^\circ$	a_i/mm	d_i/mm	$\theta_i/^\circ$
1	-90.3353	249.5765	654.2351	0.5676
2	-0.2354	899.1245	-0.2352	-90.2354
3	90.4562	-205.0254	-0.6854	180.4565
4	-90.2541	0.4568	1032.1235	0.1242
5	90.7654	-0.1235	0.1235	90.1215
6	0.1245	-0.1235	199.5464	0.7668

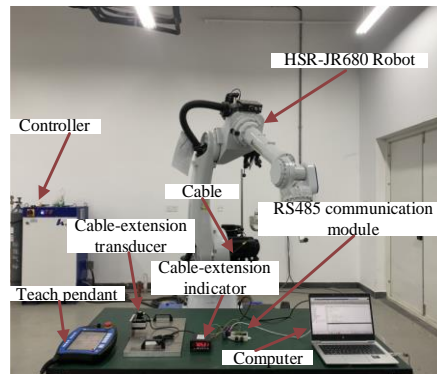


Fig. 1. Experimental system.

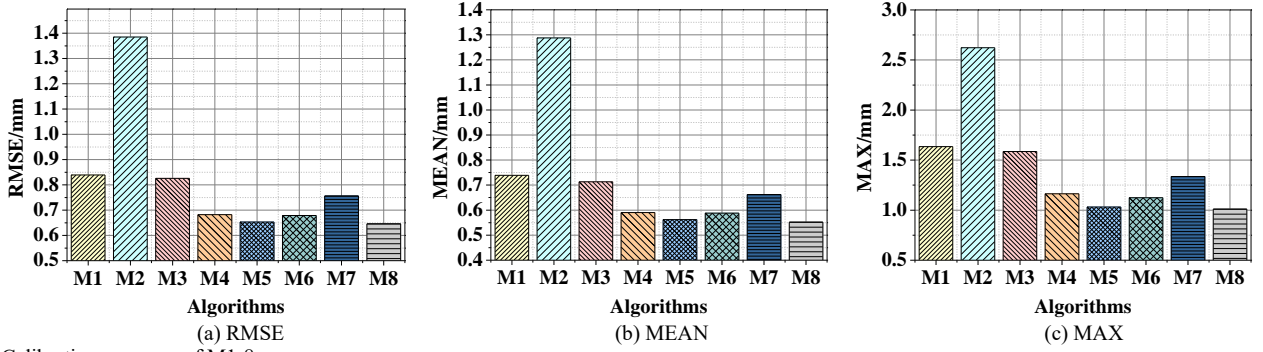


Fig. 2. Calibration accuracy of M1-8.

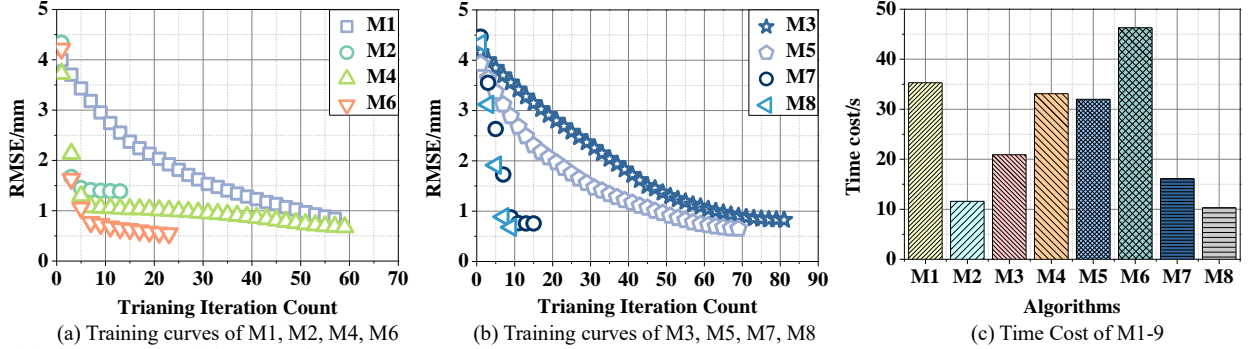


Fig. 3. Training curves and total time cost of M1-8.

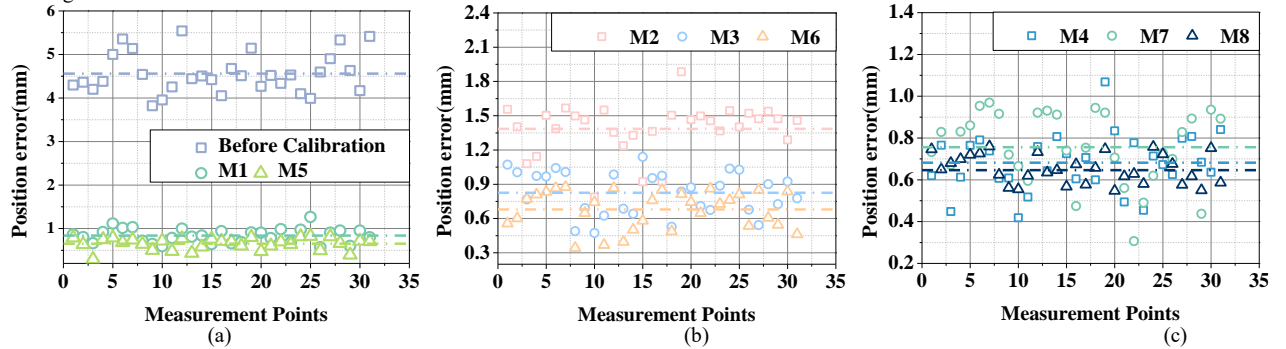


Fig. 4. The positioning accuracy of the robot after calibration through all compared algorithms. Notably, the dotted lines indicate the mean values. It shows that M8 achieves the highest positioning accuracy.

d) AdaModW can enhance positioning accuracy greatly. In this paper, 30 data points are randomly chosen from the tested datasets for a comparative analysis of position errors across M1 to M8. As shown in Fig. 4, all models are capable of substantially lowering the positioning errors in robots, among which M8 performs the best. Additionally, the deviations of the kinematic parameters optimized by M8 are acceptable and kept within limits, indicating that the accuracy gains are not attributable to overfitting.

I. CONCLUSIONS

Aiming to achieve efficient robot calibration, this paper proposes a novel AdaModW algorithm, which introduces a hyperparameter into the Adam algorithm to define the length of memory, effectively addressing the issue of the abnormal learning rate. Moreover, it interpolates a weight decay coefficient to address the inadequacy of weight decay and improve its generalization. Empirical studies on the robots show that the proposed algorithm has high calibration accuracy and convergence rate, presenting a practical approach for the field of robot calibration research. Presently, two appealing issues remain open:

- The robotic accuracy can be further increased by reducing non-geometric errors [80].
- GPU can be adopted to further enhance the computational efficiency of the AdaModW algorithm [81].

REFERENCES

- Z. Li, S. Li, A. Francis, and X. Luo, "A novel calibration system for robot arm via an open dataset and a learning perspective," *IEEE Transactions on Circuits and Systems II: Express Briefs*, vol. 69, no. 12, pp. 5169-5173, Dec. 2022.
- H. Xie, W. Li, and H. Liu, "General geometry calibration using arbitrary free-form surface in a vision-based robot system," *IEEE Transactions on Industrial Electronics*, vol. 69, no. 6, pp. 5994-6003, Jun. 2022.
- F. Bi, T. He, and X. Luo, "A fast nonnegative autoencoder-based approach to latent feature analysis on high-dimensional and incomplete data," *IEEE Transactions on Services Computing*, vol. 17, no. 3, pp. 733-746, Jun. 2024.
- X. Luo, Y. Yuan, S. Chen, N. Zeng, and Z. Wang, "Position-Transitional Particle Swarm Optimization-Incorporated Latent Factor Analysis," *IEEE Transactions on Knowledge and Data Engineering*, vol. 34, no. 8, pp. 3958-3970, 1 Aug. 2022.
- T. Chen and S. Li, "A Novel Industrial Robot Calibration Method Based on Multi-Planar Constraints," *2023 IEEE International Conference on Systems*,

Man, and Cybernetics (SMC), Honolulu, Oahu, HI, USA, 2023, pp. 4046-4051.

- [6] D. Wu, X. Luo, M. Shang, Y. He, G. Wang and X. Wu, "A data-characteristic-aware latent factor model for web services QoS prediction," *IEEE Transactions on Knowledge and Data Engineering*, vol. 34, no. 6, pp. 2525-2538, Jun. 2022.
- [7] T. Chen and S. Li, "A hybrid- L_p -norms-oriented robot kinematic calibration model optimized by a novel newton interpolated differential evolution algorithm," *2023 IEEE International Conference on Data Mining Workshops (ICDMW)*, Shanghai, China, 2023, pp. 406-411.
- [8] X. Li, W. Li, X. Yin, X. Ma, X. Yuan, and J. Zhao, "Camera-mirror binocular vision-based method for evaluating the performance of industrial robots," *IEEE Transactions on Instrumentation and Measurement*, vol. 70, pp. 1-14, Nov. 2021, Art. no. 5019214.
- [9] A. Buerkle, W. Eaton, A. Al-Yacoub, M. Zimmer, P. Kinnell, M. Henshaw, M. Coombes, W. Chen, and N. Lohse, "Towards industrial robots as a service (IRaaS): Flexibility, usability, safety and business models," *Robotics and Computer-Integrated Manufacturing*, vol. 81, Jun. 2023, Art. no. 102484.
- [10] Y. Yuan, J. Li, and X. Luo, "A fuzzy PID-incorporated stochastic gradient descent algorithm for fast and accurate latent factor analysis," *IEEE Transactions on Fuzzy Systems*, vol. 32, no. 7, pp. 4049-4061, July. 2024.
- [11] W. Qin, X. Luo, S. Li, and M. Zhou, "Parallel adaptive stochastic gradient descent algorithms for latent factor analysis of high-dimensional and incomplete industrial data," *IEEE Transactions on Automation Science and Engineering*, doi: 10.1109/TASE.2023.3267609.
- [12] N. Zeng, X. Li, P. Wu, H. Li, and X. Luo, "A novel tensor decomposition-based efficient detector for low-altitude aerial objects with knowledge distillation scheme," *IEEE/CAA Journal of Automatica Sinica*, vol. 11, no. 2, pp. 487-501, Feb. 2024.
- [13] D. Wu, P. Zhang, Y. He, and X. Luo, "MMLF: Multi-metric latent feature analysis for high-dimensional and incomplete data," *IEEE Transactions on Services Computing*, vol. 17, no. 2, pp. 575-588, Mar. 2024.
- [14] T. Chen, S. Li, and X. Luo, "A Highly-Accurate Robot Calibration Method with Line Constraint," *2023 IEEE International Conference on Networking, Sensing and Control (ICNSC)*, Marseille, France, 2023, pp. 1-6.
- [15] L. Hu, J. Zhang, X. Pan, X. Luo, and H. Yuan, "An effective link-based clustering algorithm for detecting overlapping protein complexes in protein-protein interaction networks," *IEEE Transactions on Network Science and Engineering*, vol. 8, no. 4, pp. 3275-3289, Dec. 2021.
- [16] Z. Li, S. Li and X. Luo, "Efficient Industrial Robot Calibration via a Novel Unscented Kalman Filter-Incorporated Variable Step-Size Levenberg-Marquardt Algorithm," *IEEE Transactions on Instrumentation and Measurement*, vol. 72, pp. 1-12, 2023, Art. no. 2510012.
- [17] K. Deng, D. Gao, S. Ma, C. Zhao, and Y. Lu, "Elasto-geometrical error and gravity model calibration of an industrial robot using the same optimized configuration set," *Robotics and Computer-Integrated Manufacturing*, vol. 83, Oct. 2023, Art. no. 102558.
- [18] J. Chen, F. Xie, X. J. Liu, and Z. Chong, "Elasto-geometrical calibration of a hybrid mobile robot considering gravity deformation and stiffness parameter errors," *Robotics and Computer-Integrated Manufacturing*, vol. 79, Feb. 2023, Art. no. 102437.
- [19] X. Luo, H. Wu, and Z. Li, "Neultf: a novel approach to nonlinear canonical polyadic decomposition on high-dimensional incomplete tensors," *IEEE Transactions on Knowledge and Data Engineering*, vol. 35, no. 6, pp. 6148-6166, Jun. 2023.
- [20] T. Chen, S. Li, and H. Wu, "Highly-accurate robot calibration based on plane constraint via integrating square-root cubature Kalman filter and Levenberg-Marquardt algorithm," *2022 IEEE International Conference on Networking, Sensing and Control (ICNSC)*, Shanghai, China, 2022, pp. 1-6.
- [21] Z. Li, S. Li, O. O. Bamasag, A. Alhothali, and X. Luo, "Diversified Regularization Enhanced Training for Effective Manipulator Calibration," *IEEE Transactions on Neural Networks and Learning Systems*, vol. 34, no. 11, pp. 8778-8790, Nov. 2023.
- [22] L. Hu, Y. Yang, Z. Tang, Y. He, and X. Luo, "FCAN-MOPSO: An improved fuzzy-based graph clustering algorithm for complex networks with multiobjective particle swarm optimization," *IEEE Transactions on Fuzzy Systems*, vol. 31, no. 10, pp. 3470-3484, Oct. 2023.
- [23] T. Sun, C. Liu, B. Lian, P. Wang, and Y. Song, "Calibration for precision kinematic control of an articulated serial robot," *IEEE Transactions on Industrial Electronics*, vol. 68, no. 7, pp. 6000-6009, July. 2021.
- [24] D. Wu, Y. He, and X. Luo, "A graph-incorporated latent factor analysis model for high-dimensional and sparse data," *IEEE Transactions on Emerging Topics in Computing*, vol. 11, no. 4, pp. 907-917, Oct. 2023.
- [25] Y. Zhou, C-Y. Chen, Y. Tang, H. Wan, J. Luo, G. Yang, and C. Zhang, "A comprehensive on-load calibration method for industrial robots based on a unified kinetostatic error model and gaussian process regression," *IEEE Transactions on Instrumentation and Measurement*, vol. 73, pp. 1-11, Mar. 2024, Art. no. 1003611.
- [26] Y. Zhou, X. Luo, and M. Zhou, "Cryptocurrency transaction network embedding from static and dynamic perspectives: an overview," *IEEE/CAA Journal of Automatica Sinica*, vol. 10, no. 5, pp. 1105-1121, May. 2023.
- [27] L. Ma, P. Bazzoli, P. M. Sammons, R. G. Landers, and D. A. Bristow, "Modeling and calibration of high-order joint-dependent kinematic errors for industrial robots," *Robotics and Computer-Integrated Manufacturing*, vol. 50, pp. 153-167, Apr. 2018.
- [28] W. Li, R. Wang, X. Luo, and M. Zhou, "A second-order symmetric non-negative latent factor model for undirected weighted network representation," *IEEE Transactions on Network Science and Engineering*, vol. 10, no. 2, pp. 606-618, Mar. 2023.
- [29] Z. Li, S. Li, and X. Luo, "An overview of calibration technology of industrial robots," *IEEE/CAA Journal of Automatica Sinica*, vol. 8, no. 1, pp. 23-36, Jan. 2021.
- [30] M. Chen, C. He, and X. Luo, "MNL: A highly-efficient model for large-scale dynamic weighted directed network representation," *IEEE Transactions on Big Data*, vol. 9, no. 3, pp. 889-903, June. 2023.
- [31] Z. Liu, X. Liu, Z. Cao, X. Gong, M. Tan, and J. Yu, "High precision calibration for three-dimensional vision-guided robot system," *IEEE Transactions on Industrial Electronics*, vol. 70, no. 1, pp. 624-634, Jan. 2023.
- [32] X. Xu, M. Lin, X. Luo, and Z. Xu, "HRST-LR: A hessian regularization spatio-temporal low rank algorithm for traffic data imputation," *IEEE Transactions on Intelligent Transportation Systems*, vol. 24, no. 10, pp. 11001-11017, Oct. 2023.
- [33] Y. Yuan, R. Wang, G. Yuan, and X. Luo, "An adaptive divergence-based non-negative latent factor model," *IEEE Transactions on Systems, Man, and Cybernetics: Systems*, vol. 53, no. 10, pp. 6475-6487, Oct. 2023.
- [34] C. Mao, Z. Chen, S. Li, and X. Zhang, "Separable nonlinear least squares algorithm for robust kinematic calibration of serial robots," *Journal of Intelligent & Robotic Systems*, vol. 101, no. 1, pp. 1-12, Jan. 2021.
- [35] Y. Yuan, X. Luo and M. Zhou, "Adaptive divergence-based non-negative latent factor analysis of high-dimensional and incomplete matrices from industrial applications," *IEEE Transactions on Emerging Topics in Computational Intelligence*, vol. 8, no. 2, pp. 1209-1222, Apr. 2024.
- [36] X. Jia, X. Feng, H. Yong, and D. Meng, "Weight decay with tailored Adam on scale-invariant weights for better generalization," *IEEE Transactions on Neural Networks and Learning Systems*, doi: 10.1109/TNNLS.2022.3213536.
- [37] J. Chen, R. Wang, D. Wu, and X. Luo, "A differential evolution-enhanced position-transitional approach to latent factor analysis," *IEEE Transactions on Emerging Topics in Computational Intelligence*, vol. 7, no. 2, pp. 389-401, Apr. 2023.
- [38] Y. Yuan, X. Luo, M. Shang, and Z. Wang, "A Kalman-filter-incorporated latent factor analysis model for temporally dynamic sparse data," *IEEE Transactions on Cybernetics*, vol. 53, no. 9, pp. 5788-5801, Sept. 2023.
- [39] X. Luo, Y. Zhou, Z. Liu, and M. Zhou, "Fast and accurate non-negative latent factor analysis of high-dimensional and sparse matrices in recommender systems," *IEEE Transactions on Knowledge and Data Engineering*, vol. 35, no. 4, pp. 3897-3911, Apr. 2023.
- [40] T. He, Y. Ong, L. Bai, "Learning conjoint attentions for graph neural nets". *Advances in Neural Information Processing Systems*, vol. 34, pp. 2641-2653, Dec. 2021.
- [41] D. Zhang, J. Hu, J. Cheng, Z. -G. Wu, and H. Yan, "A Novel disturbance observer based fixed-time sliding mode control for robotic manipulators with global fast convergence," *IEEE/CAA Journal of Automatica Sinica*, vol. 11, no. 3, pp. 661-672, Mar. 2024.
- [42] X. Luo, L. Wang, P. Hu, and L. Hu, "Predicting protein-protein interactions using sequence and network information via variational graph autoencoder," *IEEE/ACM Transactions on Computational Biology and Bioinformatics*, vol. 20, no. 5, pp. 3182-3194, Oct. 2023.

- [43] Z. Xie, L. Jin, and X. Luo, "Kinematics-based motion-force control for redundant manipulators with quaternion control," *IEEE Transactions on Automation Science and Engineering*, vol. 20, no. 3, pp. 1815-1828, July. 2023.
- [44] D. Wu, P. Zhang, Y. He, and X. Luo, "A double-space and double-norm ensembled latent factor model for highly accurate web service QoS prediction," *IEEE Transactions on Services Computing*, vol. 16, no. 2, pp. 802-814, Apr. 2023.
- [45] Z. Lin and H. Wu, "Dynamical representation learning for Ethereum transaction network via non-negative adaptive latent factorization of tensors," *2021 International Conference on Cyber-Physical Social Intelligence (ICCSI)*, Beijing, China, 2021, pp. 1-6.
- [46] H. Ye, J. Wu, and D. Wang, "A general approach for geometric error modeling of over-constrained hybrid robot," *Mechanism and Machine Theory*, vol. 176, Oct. 2022, Art. no. 104998.
- [47] X. Luo, Y. Zhong, Z. Wang, and M. Li, "An Alternating-Direction-Method of Multipliers-Incorporated Approach to Symmetric Non-Negative Latent Factor Analysis," *IEEE Transactions on Neural Networks and Learning Systems*, vol. 34, no. 8, pp. 4826-4840, Aug. 2023.
- [48] A. Alamdar, P. Samandi, S. Hanifeh, P. Kheradmand, A. Mirbagheri, F. Farahmand, and S. Sarkar, "Investigation of a hybrid kinematic calibration method for the "Sina" surgical robot," *IEEE Robotics and Automation Letters*, vol. 5, no. 4, pp. 5276-5282, Oct. 2020.
- [49] D. Wu, X. Luo, Y. He, and M. Zhou, "A prediction-sampling-based multilayer-structured latent factor model for accurate representation to high-dimensional and sparse data," *IEEE Transactions on Neural Networks and Learning Systems*, vol. 35, no. 3, pp. 3845-3858, Mar. 2024.
- [50] F. Bi, T. He, and X. Luo, "A two-stream light graph convolution network-based latent factor model for accurate cloud service QoS estimation," *2022 IEEE International Conference on Data Mining (ICDM)*, Orlando, FL, USA, 2022, pp. 855-860.
- [51] H. Ye, J. Wu, and T. Huang, "Kinematic calibration of over-constrained robot with geometric error and internal deformation," *Mechanism and Machine Theory*, vol. 185, July. 2023, Art. no. 105345.
- [52] T. Chen, S. Li, Y. Qiao, and X. Luo, "A robust and efficient ensemble of diversified evolutionary computing algorithms for accurate robot calibration," *IEEE Transactions on Instrumentation and Measurement*, vol. 73, pp. 1-14, Feb. 2024, Art. no. 7501814.
- [53] Z. Zhu, X. Tang, C. Chen, Wang, F. Peng, R. Yan, L. Zhou, Z. Li, and J. Wu, "High precision and efficiency robotic milling of complex parts: Challenges, approaches and trends," *Robotics and Computer-Integrated Manufacturing*, vol. 35, no. 2, pp. 22-46, Feb. 2022.
- [54] A. Peters and A. C. Knoll, "Robot self-calibration using actuated 3D sensors," *Journal of Field Robotics*, vol. 41, no. 2, pp. 327-346, Mar. 2024.
- [55] H. Zhou, T. He, Y. -S. Ong, G. Cong and Q. Chen, "Differentiable Clustering for Graph Attention," *IEEE Transactions on Knowledge and Data Engineering*, vol. 36, no. 8, pp. 3751-3764, Aug. 2024.
- [56] J. Wang, W. Li, and X. Luo, "A distributed adaptive second-order latent factor analysis model," *IEEE/CAA Journal of Automatica Sinica*, doi: 10.1109/JAS.2024.124371.
- [57] H. Wu, X. Luo, M. Zhou, M. J. Rawa, K. Sedraoui and A. Albeshri, "A PID-incorporated latent factorization of tensors approach to dynamically weighted directed network analysis," *IEEE/CAA Journal of Automatica Sinica*, vol. 9, no. 3, pp. 533-546, Mar. 2022.
- [58] H. Wu, Y. Xia, and X. Luo, "Proportional-integral-derivative-incorporated latent factorization of tensors for large-scale dynamic network analysis," *2021 China Automation Congress (CAC)*, Beijing, China, 2021, pp. 2980-2984.
- [59] K. Zhu, C. Yu, and Y. Wan, "Recursive least squares identification with variable-direction forgetting via oblique projection decomposition," *IEEE/CAA Journal of Automatica Sinica*, vol. 9, no. 3, pp. 547-555, Mar. 2022.
- [60] X. Luo, H. Wu, Z. Wang, J. Wang, and D. Meng, "A Novel Approach to Large-Scale Dynamically Weighted Directed Network Representation," *IEEE Transactions on Pattern Analysis and Machine Intelligence*, vol. 44, no. 12, pp. 9756-9773, 1 Dec. 2022.
- [61] C. Lyons, R. G. Raj, and M. Cheney, "A compound Gaussian least squares algorithm and unrolled network for linear inverse problems," *IEEE Transactions on Signal Processing*, vol. 71, pp. 4303-4316, Nov. 2023.
- [62] F. Bi, T. He, Y. Xie, and X. Luo, "Two-Stream Graph Convolutional Network-Incorporated Latent Feature Analysis," *IEEE Transactions on Services Computing*, vol. 16, no. 4, pp. 3027-3042, July. 2023.
- [63] T. He, Y. Liu, Y.S. Ong, X. Wu, and X. Luo, "Polarized message-passing in graph neural networks," *Artificial Intelligence*, vol. 331, Apr. 2024, Art. No. 104129.
- [64] J. Kwon, K. Choi, and F. C. Park, "Kino-dynamic model identification: A unified geometric approach," *IEEE Transactions on Robotics*, vol. 37, no. 4, pp. 1100-1114, Aug. 2021.
- [65] F. Yin, L. Wang, W. Tian, and X. Zhang, "Kinematic calibration of a 5-DOF hybrid machining robot using an extended Kalman filter method," *Precision Engineering*, vol. 79, pp. 86-93, Jan. 2023.
- [66] G. Luo, J. Gao, L. Zhang, D. Chen, and X. Chen, "Kinematic calibration of a symmetric parallel kinematic machine using sensitivity-based iterative planning," *Precision Engineering*, vol. 77, pp. 164-178, Jun. 2022.
- [67] X. Chen and Q. Zhan, "The kinematic calibration of an industrial robot with an improved beetle swarm optimization algorithm," *IEEE Robotics and Automation Letters*, vol. 7, no. 2, pp. 4694-4701, Apr. 2022.
- [68] C. T. Mao, S. Li, Z. W. Chen, X. Zhang, and C. Li, "Robust kinematic calibration for improving collaboration accuracy of dual-arm manipulators with experimental validation," *Measurement*, vol. 155, Apr. 2020, Art. no. 107524.
- [69] J. Ding, X. Ren, R. Luo, and X. Sun, "An adaptive and momental bound method for stochastic learning," 2019, arXiv:1910.12249.
- [70] P. Zhou, X. Xie, Z. Lin and S. Yan, "Towards understanding convergence and generalization of AdamW," *IEEE Transactions on Pattern Analysis and Machine Intelligence*, doi: 10.1109/TPAMI.2024.3382294.
- [71] Y. Yan, "Error recognition of robot kinematics parameters based on genetic algorithms," *Journal of Ambient Intelligence and Humanized Computing*, vol. 11, no. 12, pp. 6167-6176, Dec. 2020.
- [72] V. Nguyen and R. Caverly, "Cable-driven parallel robot pose estimation using extended Kalman filtering with inertial payload measurements," *IEEE Robotics and Automation Letters*, vol. 6, no. 2, pp. 3615-3622, Apr. 2021.
- [73] Y. Deng, X. Hou, B. Li, J. Wang, and Y. Zhang, "A novel method for improving optical component smoothing quality in robotic smoothing systems by compensating path errors" *Optics Express*, vol. 31, no. 19, pp. 30359-30378, Sep. 2023.
- [74] X. Luo, M. Chen, H. Wu, Z. Liu, H. Yuan, and M. Zhou, "Adjusting learning depth in nonnegative latent factorization of tensors for accurately modeling temporal patterns in dynamic QoS data," *IEEE Transactions on Automation Science and Engineering*, vol. 18, no. 4, pp. 2142-2155, Oct. 2021.
- [75] R. Jiang, M. Yang, S. Wang, and T. Chao, "An improved whale optimization algorithm with armed force program and strategic adjustment," *Applied Mathematical Modelling*, vol. 81, pp. 603-623, May. 2020.
- [76] D. D. Chen, T. M. Wang, P. J. Yuan, N. Sun, and H. Y. Tang, "A positional error compensation method for industrial robots combining error similarity and radial basis function neural network," *Measurement Science and Technology*, vol. 30, no. 12, pp. 125010, Dec. 2019.
- [77] W. Li, X. Luo, H. Yuan, and M. Zhou, "A momentum-accelerated hessian-vector-based latent factor analysis model," *IEEE Transactions on Services Computing*, vol. 16, no. 2, pp. 830-844, Apr. 2023.
- [78] L. Hu, S. Yang, X. Luo, and M. Zhou, "An algorithm of inductively identifying clusters from attributed graphs," *IEEE Transactions on Big Data*, vol. 8, no. 2, pp. 523-534, Apr. 2022.
- [79] X. Jia, X. Feng, H. Yong, and D. Meng, "Weight decay with tailored Adam o latent factor model for accurate representation to high-dimensional and sparsen scale-invariant weights for better generalization," *IEEE Transactions on Neural Networks and Learning Systems*, doi: 10.1109/TNNLS.2022.3213536.
- [80] W. Yang, S. Li, Z. Li, and X. Luo, "Highly accurate manipulator calibration via extended Kalman filter-incorporated residual neural network," *IEEE Transactions on Industrial Informatics*, vol. 19, no. 11, pp. 10831-10841, Nov. 2023.
- [81] W. Qin and X. Luo, "Asynchronous parallel fuzzy stochastic gradient descent for high-dimensional incomplete data representation," *IEEE Transactions on Fuzzy Systems*, vol. 32, no. 2, pp. 445-459, Feb. 2024.